Am J Transl Res 2023;15(8):5206-5215
www.ajtr.org /ISSN:1943-8141/AJTR0149969

Original Article

Raloxifene, a SERM targets PD-L1: an in-silico study

Chirag Chopra[1], Tenzen Yodun[2], Harpreet Singh[3], Bhupender Singh[1], Shashank K Singh[2], Umesh Goutam[1]

[1]School of Bioengineering and Biosciences, Lovely Professional University, Phagwara, Punjab, India; [2]Cancer Pharmacology Division, Indian Institute of Integrative Medicine (CSIR), Jammu, J&K, India; [3]Department of Bioinformatics, Hans Raj Mahila Maha Vidyalaya, Jalandhar, Punjab, India

Received March 4, 2023; Accepted July 31, 2023; Epub August 15, 2023; Published August 30, 2023

Abstract: Objectives: Immunotherapeutic interventions in cancer have been considerably successful and widely accepted for cancer treatment, but are costly and cannot be afforded by all patients. Because of the high cost, the pharmaceutical research groups across the world are sufficiently motivated to discover or design small molecule inhibitors to treat cancer through inhibition of the immune checkpoint proteins previously targeted with monoclonal antibodies. The presented study was designed with an aim to establish raloxifene, a selective estrogen receptor modulator (SERM) as a potential ligand of the immune checkpoint protein Programmed death ligand-1 (PD-L1). Methods: In the presented study, the *in-silico* approach was used for identifying a lead molecule against PD-L1. The hits were screened using the similarity-search method, and drug-likeliness analysis, and the leads were identified through ligand-docking using Autodock. In-vitro cytotoxicity analysis was carried out using the standard sulphorhodamine B (SRB) assay and the wound healing analysis to show the inhibition of cellular migration was performed using the standard scratch assay. Results: The *in-silico* study revealed that raloxifene showed a high drug likelihood and higher binding affinity with PD-L1 as compared to the positive control (*BMS-1166;* BMS is Bristol Myers Squibb). The binding of raloxifene was shown to occur in the same region as the FDA-approved monoclonal antibodies atezolizumab and durvalumab, indicating the potential of raloxifene for PD1/PD-L1 blockade. In the *in-vitro* studies, raloxifene showed a time-dependent reduction in IC_{50} values for the cell line HCT116 (colon cancer). The scratch assay also revealed that raloxifene significantly reduced the migratory potential of HCT-116 cells in-vitro. Conclusions: PD-L1 is a potential target of the SERM raloxifene in-silico. Overall, this study is one step further towards immune checkpoint blockade using small-molecule inhibitors.

Keywords: ADME, anticancer, autodock, immune checkpoint, in-silico, PD-L1, raloxifene, Vina

Introduction

The research on immune checkpoint proteins has opened new horizons for the development of cancer immunotherapeutics. The immune checkpoint proteins and their regulation by costimulatory proteins and inhibitory ligands provide the mechanisms to cancer cells for immune-evasion. The role of these proteins in promoting cancer spread has provided a strong rationale for targeting them for tumor regression [1-3]. Ipilimumab, a human monoclonal antibody, was specifically developed to target cytotoxic T-lymphocyte antigen 4 (CTLA-4) and received approval from the US Food and Drug Administration (USFDA) in 2011 for the treatment of metastatic melanoma [4]. Building on the success of ipilimumab, researchers explored other immune checkpoints as potential targets for inhibition. One such target of interest is the complex of programmed cell death-1 (PD-1) receptor on T-cells and its ligand, PD-L1, which is overexpressed on numerous cancer cells [5, 6]. Regrettably, the side effects of inhibiting the natural inhibitory mechanisms of the immune system have been observed clinically, resulting in adverse events such as diarrhea, rash, and hepatitis [7]. Nevertheless, the exciting field of immune checkpoint inhibitors presents a promising therapeutic option for numerous cancer patients, offering the potential for curative outcomes, particularly for those with previously poor prognoses. The binding between PD-1 and PD-L1 has an immunosuppressive effect, which cancer cells exploit to evade recognition and elimination by tumor-specific T cells targeting neo-antigens on their surface [8]. PD-L1 serves as a competitive

inhibitor of T-cell co-stimulation, functioning as a negative regulator. Prolonged exposure to PD-L1 causes T-cell exhaustion, characterized by persistent impaired effector protein function [9]. Consequently, immune cells infiltrate the tumor tissue, recognize the presence of tumors but fail to eradicate the cancer cells. Reversing the exhausted phenotype of T cells by antagonizing the interaction between PD-1 and PD-L1 allows for efficient killing of cancer cells. Antibodies that target the PD-1/PD-L1 immune checkpoint have considerably been proven to be clinically effective. However, there are concerns besides the adverse reactions. The cost of immunotherapy is high in terms of the drug cost, and hospitalization costs. The development of small-molecular weight inhibitors is expected to bring several advantages in the field of PD-1/PD-L1 immune checkpoint blockade (ICB). These advantages include lower production costs, improved stability, enhanced tumor penetration, suitability for oral administration, and elimination of concerns related to immunogenicity. However, a significant challenge lies in targeting the flat and highly hydrophobic interaction surface of PD-1/PD-L1. Overcoming this challenge is crucial for the successful development of small-molecule inhibitors in the context of PD-1/PD-L1 immune checkpoint modulation [10]. There are existing reports of small molecule inhibitors of PD-L1 such as, CA-170 [11], BMS-143, BMS-202, Aurigene-1 [12], ZE-132 [13], 17 [14], INCB086550 [15], and curcumin among others [16].

Methods

In-silico validation

Retrieval and preparation of protein for docking

The three dimensional (3D) structure of the PD-L1 bound to a small inhibitor was retrieved from the Protein Data Bank (PDB) using the specific PDB ID 6R3K. To prepare the protein structure for docking with the ligand, certain steps were undertaken. These included eliminating water molecules, incorporating hydrogen atoms to ensure proper ionization and tautomeric states, and eliminating the ligand along with its heteroatoms.

Preparation of ligand for docking

The ligand molecules were retrieved using ChemMine software's Pubchem similarity search feature. 'SMILES' (Simplified Molecular Input Line Entry System) format of the input, canonical for PubChem ID: 118434635 (BMS-1166) was given. The chosen algorithm was the 'fingerprint algorithm' at a cut-off of 0.5. Similar hits were generated by ChemMine in the structured data file (SDF) format. The input SMILES format of known PD-1/PD-L1 interaction inhibitor BMS-1166 was as follows.

CC1=C(C=CC=C1COC2=C(C=C(C(=C2)OC-C3=CC=CC(=C3)C#N)CN4CC(CC4C(=O)O)O)Cl)C5=CC6=C(C=C5)OCCO6.

BMS-1166 and those structurally similar to BMS-1166 were prepared for docking using the standard Autodock tools.

ADME analysis

Analysis of absorption, distribution, metabolism, and excretion (ADME) is a vital component of any drug design study. ADME analysis was performed using SwissADME server (http://www.swissadme.ch/). The ADME data were analyzed for drug likeliness (of Lipinski's rule of 5 and bioavailability score), pharmacokinetic parameters (GI absorption, blood-brain barrier permeability, CYP inhibition, and PGP activity), and water solubility {Log S (ESOL)}.

Protein-ligand docking

The PD-L1 structure was docked with the ligands using the Autodock Vina software, with an exhaustiveness value of 8.0.

Docking analysis

Protein-ligand docking was analyzed using the parameter of binding energies of the compound in comparison with the well-established control, BMS-1166. Also, mapping of the precise residues involved in the interaction of the inhibitor with PD-L1 was performed using the PLIP (Protein-Ligand Interaction Profiler; https://plip-tool.biotec.tu-dresden.de/plip-web/plip/index) server. The images showing the binding between raloxifene and PD-L1 were generated using the Discovery Studio® [17].

Table 1. Showing ADME analysis of Raloxifene

Molecule	Raloxifene
MW	473.58
#H-bond acceptors	5
#H-bond donors	2
ESOL Log S	-6.61
ESOL Class	Poorly soluble
GI absorption	High
BBB permeant	No
Pgp substrate	Yes
CYP1A2 inhibitor	No
CYP2C19 inhibitor	Yes
CYP2C9 inhibitor	No
CYP2D6 inhibitor	Yes
CYP3A4 inhibitor	No
Lipinski #violations	0
Bioavailability Score	0.55

ADME: absorption, distribution, metabolism, and excretion.

In-vitro validation

Cell culture and media: HCT116 (human colon carcinoma) cells were used in the study for evaluating the growth inhibitory potential of raloxifene. The cells were cultured in RPMI-1640 supplemented with 10% (v/v) fetal bovine serum (South American) and Penicillin/streptomycin/amphotericin B.

Cytotoxicity analysis: Raloxifene was evaluated for their cytotoxic potential using the SRB assay as described previously [18]. HCT116 cells were seeded at a density of 7500 cells per well. The cells were then treated or untreated with varying concentrations of the drug (ranging from 0.5 μM to 50 μM), for 24 hours, 48 hours, and 72 hours.

Wound-healing assay: The wound healing assay is one of the standard assays for investigating the cell migration [19]. HCT-116 cells were seeded in 12-well plates at a density of 0.25 million cells per well and cultured till >80% confluence. The scratch was made using a p200 pipette tip at t=0 hour and the cells were washed with PBS. The cells were then treated or untreated with varying concentrations of Raloxifene (5 μM, 10 μM, 20 μM, 30 μM, and 50 μM). The positive control used in the experiment was 10 uM 5-fluorouracil. The cells were incubated for 48 hours and the plates were photographed at t=0 hour, 24 hours, and 48 hours. The efficacy of raloxifene was expressed in terms of mean percentage wound healed as compared to the untreated control.

Results and Discussion

The search for small molecule inhibitors has eluded cancer researchers since the application of immunotherapy in cancers. The BMS class of compounds has been proven to strongly bind to the key immune checkpoint protein PD-L1. However, the use of these compounds in therapy is limited due to high molecular weight and poor-to-moderate solubility. Previous research shows that other molecules have been used for targeting the PD-L1 protein for degradation, altered expression, and inhibition of PD-1/PD-L1 interaction. Work of Lim SO et al. showed that curcumin inhibited the stability of PD-L1 through inhibition of Constitutive Photomorphogenesis 9 (COP9) signalosome 5 (CSN5). CSN5 is a known inhibitor of PD-L1 degradation by ubiquitination [16]. Small molecule inhibitors such as BMS-202, and CA-170 are also reported to inhibit PD-1/PD-L1 interaction [11, 20]. AUPM-170 is also reported as a dual antagonist of PD-L1 and VISTA (V-domain immunoglobulin suppressor of T cell activation) signaling [21]. Besides inhibiting PD-1/PD-L1 interaction, some inhibitors are also known to alter the expression of PD-L1. One such compound Platycodin D induces the release of PD-L1 into the extracellular medium in-vitro. This is one potential mechanism of action of the immunomodulatory small molecules against PD-L1 as the release of PD-L1 could lead to reduced PD-1/PD-L1 signaling [22].

ADME analysis

Absorption, distribution, metabolism, and excretion are analyzed using the Swiss-ADME webserver. Using this server, the drug-likeliness (Lipinski's rule of 5 and bioavailability score), pharmacokinetic parameters (GI absorption, blood-brain barrier permeability, CYP inhibition, and PGP activity), and water solubility {Log S (ESOL)} were estimated. The results have been summarized in **Table 1**.

Table 2. 3D structure of ligands used for protein docking analysis

S. No.	Name of the Ligand	Pubchem ID	Ligand Structure
1	BMS-1166	118434635	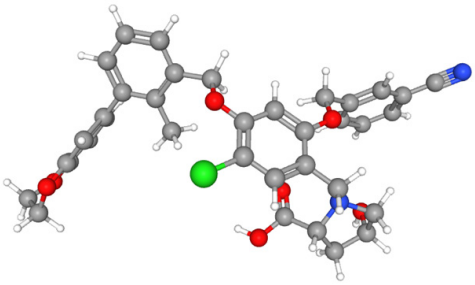
2	Raloxifene	5035	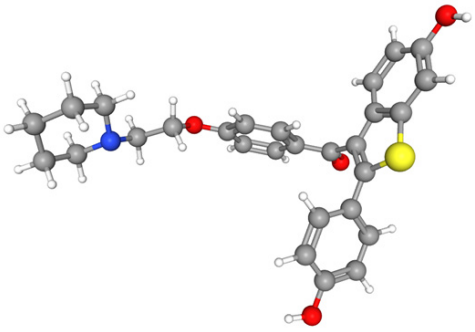

Table 3. Show the binding affinities of BMS-1166 and Raloxifene with PD-L1

Mode	Affinity (kcal/mol)	Affinity (kcal/mol)
	BMS-1166	Raloxifene
1	-6.1	-7.5
2	-5.6	-7.3
3	-5.2	-7.0
4	-4.8	-6.9
5	-4.7	-6.8
6	-4.7	-6.7
7	-3.9	-6.6

PD-L1: Programmed death ligand-1.

Docking analysis

In the present study, raloxifene and BMS-1166 (positive control) were docked with the 3D structure of PD-L1 (PDB ID 6R3K) using Autodock Vina. The 3D structure of the ligand used for docking are shown in **Table 2**.

The binding affinities of PD-L1 with BMS-1166 and raloxifene were compared using the docking score, which is estimated in kcal/mol. In this analysis, the seven best docking modes were chosen for comparison. The comparative analysis is summarized in **Table 3**.

The docking score revealed that raloxifene showed better affinity (more negative docking score) towards PD-L1 as compared to the known ligand BMS-1166. The best docking pose (PDB format) was analyzed using the PLIP server and the results obtained for BMS116 and raloxifene have been tabulated in **Table 4**.

The docked 3D structure of BMS-1166 and raloxifene with PD-L1 are shown in **Figures 1** and **2** respectively. The BMS-1166 formed two hydrogen bonds with PD-L1 amino acids Glu31 (bond length 2.3Å) and Thr37 (bond length 3.1Å). On the other hand, raloxifene formed four H-bonds with PD-L1 amino acids Ala121 (bond length 3.2Å), Asp122 (bond length 3.79Å), and Arg125 (bond lengths 3.2Å and 3.3Å).

Analysis of interaction between ligands and PD-L1

PD-L1 is the ligand for the programmed death receptor 1 (PD-1). BMS-1166 is a known ligand of PD-L1 which blocks PD-L1 function through interference with the export of PD-L1 from the endoplasmic reticulum [23]. The structural features of PD-L1 include different domains the most notable of which is the Ig-like domain,

Table 4. Show the interaction data between PD-L1 and Raloxifene, and PD-L1 and BMS-1166 (PLIP Output). All distances are shown in Angstroms

Raloxifene														
Hydrophobic Interactions							Hydrogen Bonds							
Index	Chain	Residue	Amino Acid	Distance	Ligand Atom	Protein Atom	Index	Chain	Residue	Amino Acid	Distance H-A*	Distance D-A**	Donor Atom	Acceptor Atom
1	B	54	Ile	3.95	3887	1244	1	A	121	Ala	2.25	3.20	3884 [N3]	794 [02]
2	B	56#	Tyr	3.48	3888	1259	2	A	122	Asp	3.44	3.79	802 [03]	3884 [N3]
3	B	63	Asn	3.68	3892	1323	3	A	125#	Arg	2.51	3.31	825 [Nam]	3898 [03]
4	B	66	Gln	3.78	3887	1348	4	A	125#	Arg	3.16	3.65	835 [Ng+]	3898 [03]
6	A	124#	Lys	3.65	3871	822								
7	A	125#	Arg	3.81	3871	830								
BMS-1166														
Hydrophobic Interactions							Hydrogen Bonds							
Index	Chain	Residue	Amino Acid	Distance	Ligand Atom	Protein Atom	Index	Chain	Residue	Amino Acid	Distance H-A*	Distance D-A**	Donor Atom	Acceptor Atom
1	B	24	Pro	3.72	3907	1019	1	B	31	Glu	2.30	3.22	3891 [03]	1080 [0.C02]
2	B	30	Val	3.67	3869	1070	2	B	37	Thr	2.25	3.11	1119 [NAM]	3864 [N3]
4	B	36	Met	3.95	3870	1115								
5	C	134	Tyr	3.71	3901	2823								
6	C	134	Tyr	3.99	3880	2819								
7	C	134	Tyr	3.42	3876	2818								

#Interacting residues with raloxifene that match the interacting residues with atezolizumab and durvalumab. *H-A = Distance between Hydrogen and Acceptor Atom. **D-A = Distance between Donor and Acceptor Atom. PD-L1: Programmed death ligand-1.

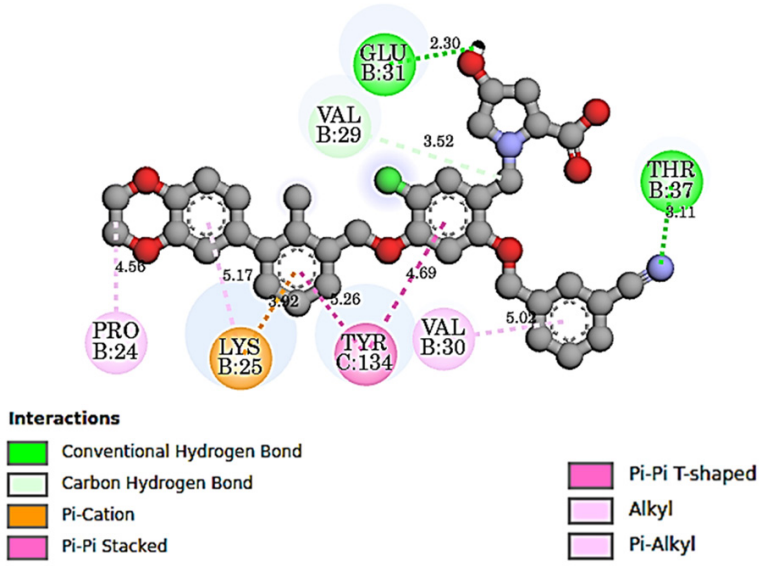

Figure 1. The image shows the interacting amino acids of PD-L1 with BMS-1166. All bond distances are shown in Angstroms. PD-L1: Programmed death ligand-1.

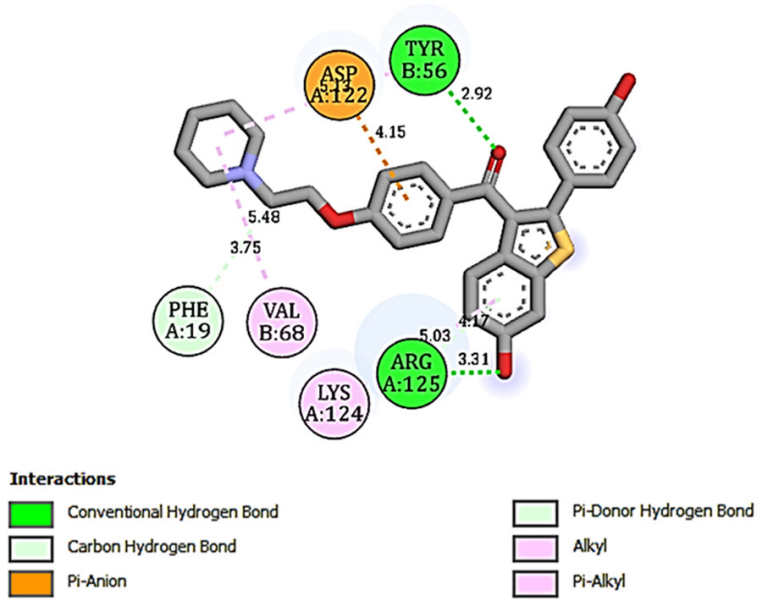

Figure 2. The image shows the interacting amino acids of PD-L1 with Raloxifene. All bond distances are shown in Angstroms. PD-L1: Programmed death ligand-1.

besides the transmembrane domain (Tm) and the RNApol-like domain. PD-L1 has a typical structure belonging to the immunoglobulin (Ig) superfamily of proteins [24]. Several pro-inflammatory signals are known to activate PD-L1 expression, however, PD-L1 is constitutively expressed in macrophages, dendritic cells, and myeloid-derived suppressor cells [25]. Raloxifene is a SERM prescribed as a medication to treat osteoporosis in postmenopausal women [26]. It is a non-steroidal drug that is known to increase bone mineral density. Raloxifene is also an anti-cancer drug, especially used for breast cancer as an estradiol antagonist that competes for binding with estrogen receptors. Protein-ligand docking showed the binding of raloxifene with PD-L1 (6R3K) at some important amino acid residues. Raloxifene formed hydrophobic interactions with the amino acids I54, Y56, N63, Q66, V68 (all on chain-B), and K124 (on chain-A). Raloxifene also showed H-bonding with A121, D122, and R125. Interestingly, Lee et al. showed that the residues Y56, N63, Q66, and V68 are also the contact amino acids for binding of FDA-approved Atezolizumab with PD-L1. Also, A121 and R125 are known as contact residues between atezolizumab and PD-L1. Atezolizumab is a known monoclonal antibody for PD-1/PD-L1 blockade. Additionally, Y56, A121, K124, and R125 are contact residues between PD-L1 and FDA-approved durvalumab, which is again a known PD1/PD-L1 blockade agent [27]. This overlap is a positive indication that raloxifene may potentially inhibit PD1/PD-L1 signaling.

In-vitro cytotoxicity analysis

The in-vitro cytotoxicity analysis was carried out on human cancer cell line (human colon cancer). Previous reports have shown that the cell lines HCT116 and colon cancer stem cells express PD-L1 [28, 29]. The cytotoxicity analy-

Table 5. Show the percentage growth inhibition and MCF-7 and HCT116 cells and IC_{50} values in response to varying dosages of Raloxifene for different time points

Drug	Cell Line	Concentration (μM)	Percentage Growth Inhibition			IC_{50}		
			24 hours	48 hours	72 hours	24 hours	48 hours	72 hours
Raloxifene	HCT116	Untreated	0.00	0.00	0.00	29.54 μM	19.56 μM	12.39 μM
		0.5	3.44±1.36	5.48±2.32	14.42±5.53			
		1	4.03±3.15	7.97±3.79	23.92±3.82			
		5	5.84±0.68	15.34±3.74	26.22±11.32			
		10	9.15±4.58	26.67±3.46*	44.04±3.15*			
		20	29.16±4.13**	65.84±1.28**	91.01±0.67**			
		30	56.76±1.21**	91.41±0.09**	91.55±0.51			
		50	85.04±3.37*	95.53±0.19	92.47±0.39			

*p-value <0.05; **p-value <0.01 (paired t-test was performed for studying the effect of dose on the percentage growth inhibition).

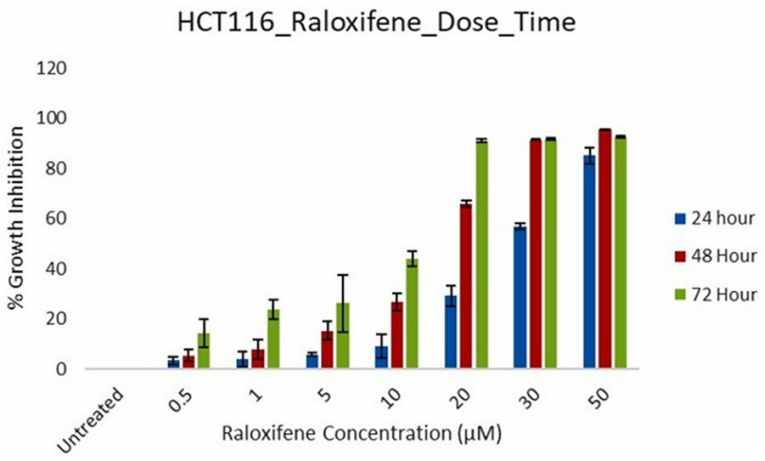

Figure 3. The image graphically represents the percentage inhibition of HCT116 and MCF-7 in response to varying dosage of Raloxifene for 24 hours, 48 hours, and 72 hours.

sis was done through a dose-dependent and time-dependent study. The cells were cultured in T-75 flasks, trypsinized, and seeded in flat-bottom 96-well cell culture plates. Treatment was given at varying doses for 24 hours, 48 hours, and 72 hours.

It was seen that raloxifene significantly inhibited the growth of HCT116 cells in-vitro. The IC_{50} values and the percentage growth inhibition are summarized in **Table 5** and represented graphically in **Figure 3**.

The study revealed that 24-hour treatment with raloxifene showed an IC_{50} value of 29.54 micromolar for HCT116. The IC_{50} of raloxifene was reduced in a time-dependent manner and 72-hour treatment showed the highest growth inhibition. This result corroborates with the available research data. For HCT116, the observed IC_{50} value of 29.54 micromolar corroborates with the available research reports. Abd-Rabou et al. reported that raloxifene killed HCT116 cells in-vitro with an IC_{50} value of 28.7 micromolar [30]. At 48 hours, our study reported a raloxifene IC_{50} of 19.56 micromolar. Tu et al. reported nearly 50 percent inhibition of HCT116 cell growth after 48 hours at raloxifene dose of 20 micromolar (data extracted from graph) [31].

Wound-healing assay

The effect of raloxifene on HCT116 cell migration was studied using the standard scratch assay. The cells were treated or untreated with varying concentrations of raloxifene along with ten micromolar 5-fluorouracil as a positive control. The images were taken at t=0 hour, 24 hours and 48 hours and the results are shown in **Figure 4** and tabulated in **Table 6**. It was seen that raloxifene showed time and dose-dependent reduction of wound healing as measured through the mean area of the open wound. The results showed that the 99.45% of the wound of the untreated cells healed at 48 hours, whereas, treatment with 5 μM, 10 μM, 20 μM, 30 μM and 50 μM raloxifene showed a mean percentage wound healing of 31.2%,

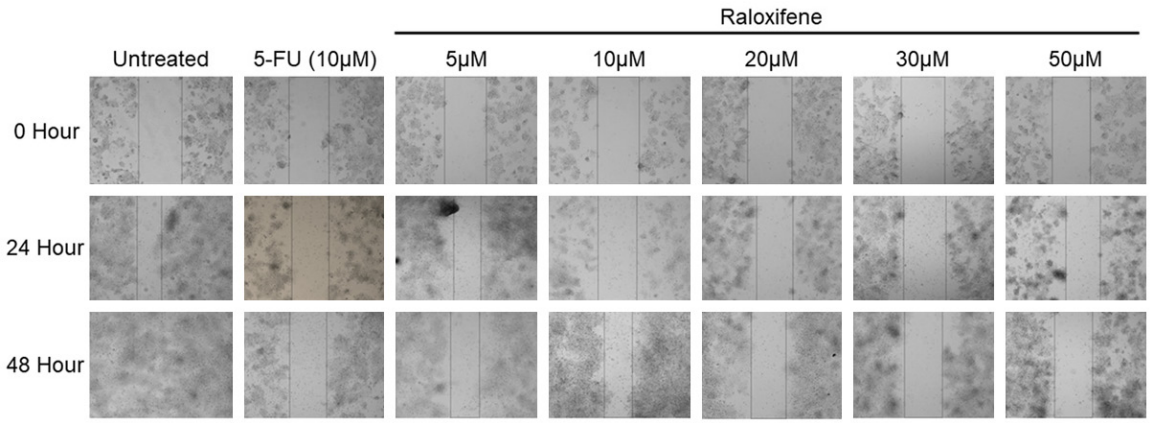

Figure 4. The image shows the representative images of the wound healing assay on HCT116 cells with or without treatment with raloxifene and 5-fluorouracil (10 micromolar).

Table 6. Show the percentage wound healing in HCT-116 cells in response to varying concentrations of raloxifene, untreated control and 5-fluorouracil (10 μM)

Incubation Time	Percentage Wound Healed						
	Untreated	5-FU (10 μM)	Raloxifene (5 μM)	Raloxifene (10 μM)	Raloxifene (20 μM)	Raloxifene (30 μM)	Raloxifene (50 μM)
0 hour	0	0	0	0	0	0	0
24 hour	36.03±1.09**	0.88±1.57	33.84±6.54*	12.93±1.40*	10.10±1.98	2.55±5.45	2.30±3.87
48 hour	99.45±1.98**	4.41±2.42	31.20±1.96	25.21±0.79**	19.27±0.83**	12.03±3.64	0

*p-value <0.05; **p-value <0.01 (paired t-test was performed for studying the effect of dose on the percentage wound healing).

25.2%, 19.27%, 12.03% and 0% respectively at 48 hours. This confirms the inhibitory potential of raloxifene against cancer cell migration.

Conclusion

The in-silico findings of this study show that raloxifene is a potent inhibitor for PD-L1 and can potentially target the PD1/PD-L1 signaling pathway by inhibiting their interaction. Raloxifene is an already reported SERM and is applicable to cancer research. However, this is the first report of the efficacy of raloxifene in PD1/PD-L1 blockade. The amino acids of PD-L1 that are targeted by raloxifene overlap those that are targeted by atezolizumab and durvalumab, which implies that a low-cost inhibitor like raloxifene can benefit the patients who cannot afford the expensive immunotherapy. The quest for small-molecule inhibitors for immune checkpoint blockade has been going on for some time now and with further structural biology experimentation, the efficacy of binding of such inhibitors to high-value therapeutic targets can be proven. More research is required to get more insights into the mechanism of cell death by raloxifene through targeting of PD-L1. Much remains to be determined as to whether raloxifene inhibits PD-1/PD-L1 interaction, alters PD-L1 expression, or its stability. This paper provides the necessary impetus to pursue the interaction between raloxifene and PD-L1 further and explore the possibilities of development of effective drug combinations.

Acknowledgements

The authors thank the management of LPU for providing the Computational Biology facility for in-silico work. Harpreet Singh acknowledges the research grant from the Department of Science and Technology, Government of India, for the development of computational resources ("Fund for Improvement of Science and Technology Infrastructure (FIST)" grant D. O. No. SR/FST/PG College/2009).

Disclosure of conflict of interest

None.

Address correspondence to: Umesh Goutam, School of Bioengineering and Biosciences, Lovely Professional University, Phagwara, Punjab, India. E-mail: umeshbiotech@gmail.com; Shashank K Singh, Cancer Pharmacology Division, Indian Institute of Integrative Medicine (CSIR), Jammu, J&K, India. E-mail: sksingh@iiim.ac.in

References

[1] Ishida Y, Agata Y, Shibahara K and Honjo T. Induced expression of PD-1, a novel member of the immunoglobulin gene superfamily, upon programmed cell death. EMBO J 1992; 11: 3887-95.

[2] Krummel MF and Allison JP. CD28 and CTLA-4 have opposing effects on the response of T cells to stimulation. J Exp Med 1995; 182: 459-65.

[3] Leach DR, Krummel MF and Allison JP. Enhancement of antitumor immunity by CTLA-4 blockade. Science 1996; 271: 1734-6.

[4] Lipson EJ and Drake CG. Ipilimumab: an anti-CTLA-4 antibody for metastatic melanoma. Clin Cancer Res 2011; 17: 6958-62.

[5] Ostrand-Rosenberg S, Horn LA and Haile ST. The programmed death-1 immune-suppressive pathway: barrier to antitumor immunity. J Immunol 2014; 193: 3835-41.

[6] Dong P, Xiong Y, Yue J, Hanley SJB and Watari H. Tumor-intrinsic PD-L1 signaling in cancer initiation, development and treatment: beyond immune evasion. Front Oncol 2018; 8: 386.

[7] Winer A, Bodor JN and Borghaei H. Identifying and managing the adverse effects of immune checkpoint blockade. J Thorac Dis 2018; 10 Suppl 3: S480-S489.

[8] Waldman AD, Fritz JM and Lenardo MJ. A guide to cancer immunotherapy: from T cell basic science to clinical practice. Nat Rev Immunol 2020; 20: 651-68.

[9] Wherry EJ and Kurachi M. Molecular and cellular insights into T cell exhaustion. Nat Rev Immunol 2015; 15: 486-99.

[10] Skalniak L, Zak KM, Guzik K, Magiera K, Musielak B, Pachota M, Szelazek B, Kocik J, Grudnik P, Tomala M, Krzanik S, Pyrc K, Dömling A, Dubin G and Holak TA. Small-molecule inhibitors of PD-1/PD-L1 immune checkpoint alleviate the PD-L1-induced exhaustion of T-cells. Oncotarget 2017; 8: 72167-72181.

[11] Powderly J, Patel MR, Lee JJ, Brody J, Meric-Bernstam F, Hamilton E, Aix SP, Garcia-Corbacho J, Bang YJ and Ahn MJ. CA-170, a first in class oral small molecule dual inhibitor of immune checkpoints PD-L1 and VISTA, demonstrates tumor growth inhibition in pre-clinical models and promotes T cell activation in Phase 1 study. Ann Oncol 2017; 28: v405-6.

[12] Ganesan A, Ahmed M, Okoye I, Arutyunova E, Babu D, Turnbull WL, Kundu JK, Shields J, Agopsowicz KC, Xu L, Tabana Y, Srivastava N, Zhang G, Moon TC, Belovodskiy A, Hena M, Kandadai AS, Hosseini SN, Hitt M, Walker J, Smylie M, West FG, Siraki AG, Lemieux MJ, Elahi S, Nieman JA, Tyrrell DL, Houghton M and Barakat K. Comprehensive in vitro characterization of PD-L1 small molecule inhibitors. Sci Rep 2019; 9: 12392.

[13] Liu C, Zhou F, Yan Z, Shen L, Zhang X, He F, Wang H, Lu X, Yu K, Zhao Y and Zhu D. Discovery of a novel, potent and selective small-molecule inhibitor of PD-1/PD-L1 interaction with robust in vivo anti-tumour efficacy. Br J Pharmacol 2021; 178: 2651-70.

[14] Wang T, Cai S, Cheng Y, Zhang W, Wang M, Sun H, Guo B, Li Z, Xiao Y and Jiang S. Discovery of small-molecule inhibitors of the PD-1/PD-L1 axis that promote PD-L1 internalization and degradation. J Med Chem 2022; 65: 3879-93.

[15] Koblish HK, Wu L, Wang LS, Liu PCC, Wynn R, Rios-Doria J, Spitz S, Liu H, Volgina A, Zolotarjova N, Kapilashrami K, Behshad E, Covington M, Yang YO, Li J, Diamond S, Soloviev M, O'Hayer K, Rubin S, Kanellopoulou C, Yang G, Rupar M, DiMatteo D, Lin L, Stevens C, Zhang Y, Thekkat P, Geschwindt R, Marando C, Yeleswaram S, Jackson J, Scherle P, Huber R, Yao W and Hollis G. Characterization of INCB086550: a potent and novel small-molecule PD-L1 inhibitor. Cancer Discov 2022; 12: 1482-1499.

[16] Lim SO, Li CW, Xia W, Cha JH, Chan LC, Wu Y, Chang SS, Lin WC, Hsu JM, Hsu YH, Kim T, Chang WC, Hsu JL, Yamaguchi H, Ding Q, Wang Y, Yang Y, Chen CH, Sahin AA, Yu D, Hortobagyi GN and Hung MC. Deubiquitination and stabilization of PD-L1 by CSN5. Cancer Cell 2016; 30: 925-39.

[17] Studio D. Discovery studio. Accelrys [21]. 2008.

[18] Vichai V and Kirtikara K. Sulforhodamine B colorimetric assay for cytotoxicity screening. Nat Protoc 2006; 1: 1112-6.

[19] Liang CC, Park AY and Guan JL. In vitro scratch assay: a convenient and inexpensive method for analysis of cell migration in vitro. Nat Protoc 2007; 2: 329-33.

[20] Chupak LS and Zheng X. Compounds useful as immunomodulators. Google Patents; 2018.

[21] Sasikumar P, Sudarshan N, Gowda N, Samiulla DS, Ramachandra RK, Chandrasekhar T, Adurthi S, Dhudashia AA, Gowda N and Ramachandra M. AUPM-170: first-in-class, oral immune checkpoint inhibitor of PD-L1/2 and VISTA. In: AACR annual meeting. 2015.

[22] Huang MY, Jiang XM, Xu YL, Yuan LW, Chen YC, Cui G, Huang RY, Liu B, Wang Y, Chen X and Lu JJ. Platycodin D triggers the extracellular re-

lease of programed death Ligand-1 in lung cancer cells. Food Chem Toxicol 2019; 131: 110537.
[23] Chen FF, Li Z, Ma D and Yu Q. Small-molecule PD-L1 inhibitor BMS1166 abrogates the function of PD-L1 by blocking its ER export. Oncoimmunology 2020; 9: 1831153.
[24] Escors D, Gato-Cañas M, Zuazo M, Arasanz H, García-Granda MJ, Vera R and Kochan G. The intracellular signalosome of PD-L1 in cancer cells. Signal Transduct Target Ther 2018; 3: 26.
[25] Lu C, Redd PS, Lee JR, Savage N and Liu K. The expression profiles and regulation of PD-L1 in tumor-induced myeloid-derived suppressor cells. Oncoimmunology 2016; 5: e1247135.
[26] Scott JA, Da Camara CC and Early JE. Raloxifene: a selective estrogen receptor modulator. Am Fam Physician 1999; 60: 1131-9.
[27] Lee HT, Lee JY, Lim H, Lee SH, Moon YJ, Pyo HJ, Ryu SE, Shin W and Heo YS. Molecular mechanism of PD-1/PD-L1 blockade via anti-PD-L1 antibodies atezolizumab and durvalumab. Sci Rep 2017; 7: 5532.
[28] Jian L, Zhicheng H and Shubai L. Polysaccharide peptide induced colorectal cancer cells apoptosis by down-regulating EGFR and PD-L1 expression. Iran J Pharm Res 2022; 21: e123909.
[29] Wu Y, Chen M, Wu P, Chen C, Xu ZP and Gu W. Increased PD-L1 expression in breast and colon cancer stem cells. Clin Exp Pharmacol Physiol 2017; 44: 602-4.
[30] Abd-Rabou AA, Mwaheb MA and Kishta MS. 5-fluorouracil synergized with raloxifene and cytosineβ-D-arabinofuranoside to combat colorectal cancers in vitro via controlling lipolysis. J Pharmacol Toxicol 2016; 12: 14-32.
[31] Tu Z, Ma Y, Tian J, Li H, Akers W, Achilefu S and Gu Y. Estrogen receptor β potentiates the antiproliferative effect of raloxifene and affects the cell migration and invasion in HCT-116 colon cancer cells. J Cancer Res Clin Oncol 2012; 138: 1091-103.